Industrial Crops & Products 223 (2025) 120163

Contents lists available at ScienceDirect

Industrial Crops & Products

journal homepage: www.elsevier.com/locate/indcrop

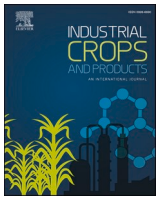

# Effect of biochar content and particle size on mechanical and water absorption properties of landscaping waste/polylactic acid composites

Ruyan Zhang [a], Haixin Peng [b], Shenhao Li [a], Xia Yang [a], Hongbo Li [c], Zebing Xing [c], Yu Xian [a,*]

[a] College of Forestry, Shanxi Agricultural University, Taigu, Shanxi 030801, China
[b] Department of Biosystems Engineering, College of Engineering Auburn University, Auburn 36849, USA
[c] College of Agricultural Engineering, Shanxi Agricultural University, Taigu, Shanxi 030801, China

ARTICLE INFO

*Keywords:*
Landscaping waste
Biochar
Composites
Mechanical properties
Water absorption

ABSTRACT

The high-value utilization of landscaping waste to produce wood-plastic composites provides a promising approach to waste management, yet remains a challenge. In this study, wood-plastic composites were prepared using landscaping waste and polylactic acid (PLA) through an extrusion-molding process, with biochar (BC) as the reinforcing material. First, the effects of biochar content (0.5 %, 1 %, 2 %, 3 %, 4 %) and particle size (100mesh, 300mesh, 800mesh, 1200 mesh) on the physico-mechanical and dynamic thermo mechanical properties of the composites were analyzed. A multivariate nonlinear model was employed to fit the flexural properties of the composites. Additionally, the water absorption properties were investigated under immersion conditions at three different temperatures (20°C, 35°C, 50°C). The results demonstrated that biochar significantly improved the interfacial compatibility between landscaping waste and PLA, enhancing the mechanical properties of this composite. When the biochar content was 1 % and particle size was 100 mesh, flexural strength reached 25.16 MPa, respectively, representing increases of 19.20 % over composites without biochar, while the change in impact strength was small. In addition, the water absorption process of composites with 1 % BC were well fitted by Fick's law. SEM morphology observation indicated that interfacial bonding was reduced after water absorption, which was consistent with the test results. Combined with Arrhenius equation and Fick's law, the water absorption model of the composites at each water immersion temperature was obtained, which can predict the water absorption behavior at 60°C.

## 1. Introduction

Waste management and utilization are cornerstones of urban landscaping. In recent decades, the rapid growth of garden waste has become a major sources of municipal solid wastes, causing increasingly serious environmental problems. Green waste includes shrub prunings, fallen leaves, dead branches, and pine straw (Bai et al., 2010). Effective and systematic garden greening can help alleviate environment stress, and benefit human health (Song, 2020). Currently, there are two traditional treatment methods, landfill or incineration (An, 2020; Mølgaard, 1995). Landfill takes up a lot of land. Moreover, the precise mechanisms by which biochemical and microbial reactions occur are not yet well understood. Researchers have shown that traditional composting treatment can utilize landscaping waste (LW), but is limited by technology, offers low added value, and is difficult to market (Mokhtar et al., 2022). Therefore, there is an urgent need for more environment friendly and sustainable waste treatment. Regarding LW, the development of new biodegradable composites has become a key research focus and is attracting constant interest.

In this context, wood plastic composites (WPC), a new type of green and recyclable material based on natural plant fibers, will meet the eco-friendly requirements They are manufactured with fiber fillers and thermoplastic polymer materials through various processing methods, such as melt extrusion, thermopressure compounding, and injection molding (Friedrich, 2021; Xian et al., 2022). Because it retains the appearance of plant fibers and high performance, it is now widely used in landscape architecture(Ratanawilai and Srivabut, 2021), jetty (Fortini, 2018) ornamental (Zhang et al., 2021)and other fields. Traditional WPCs typically contain polyethylene PE, polypropylene PP and other non-degradable plastic products (Ma et al., 2024). Instead, polylactic acid PLA is a biocompatible and sustainably processable material. Its wide availability and durable properties have sparked great interest

* Corresponding author.
*E-mail address:* xianyu_sxau@126.com (Y. Xian).

https://doi.org/10.1016/j.indcrop.2024.120163
Received 5 September 2024; Received in revised form 11 November 2024; Accepted 27 November 2024
Available online 3 December 2024

in research and application.(Jamshidian et al., 2010; Rajeshkumar et al., 2021). According to previous reports, however, the use of PLA has the disadvantage of low thermal stability and high costs (Chong et al., 2021; Martinez Villadiego et al., 2022). In addition, poor interfacial compatibility within plant fibers has limited the application of PLA-based wood composites. To address these issues, many researchers are working on modification methods to improve performance. Saeed et al. reported that fusabond (FB)was utilized as an interfacial modifier to reinforce composites based on PLA and jute fiber (JF), the blending of 30 % JF and 3 % FB significantly improved tensile strength and other thermo-mechanical properties, as well as interfacial adequacy between PLA and jute fibers (Saeed et al., 2023). Similarly, Ramesh et al. investigated PLA, Aloe vera fibers and montmorillonite clay to produce compression-molded reinforced nanobiocomposites, where montmorillonite clay at 1 % by weight enhanced tensile strength over control group (Ramesh et al., 2020). Howerver, montmorillonite tended to aggregate and had poor dispersion, limiting its application and performance.

Biochar has proved to be a multifunctional carbon material with a high specific surface area, and low cost. It is formed by the high-temperature pyrolysis of biomass waste, such as poultry manure, wood wastes, and agricultural residues (Wang et al., 2023; Yi et al., 2020). George et al. produced a polylactic acid/polybutylene adipate-co-terephthalate composites with biochar for antistatic applications, and found that 1 wt% biochar increased the tensile strength of PLA/PBAT materials (George et al., 2023). In another study, the researcher used bamboo charcoal (BC) as a reinforcing material. The biochar formed strong interfacial interactions that improved the composite's flextural properties (Li et al., 2014).These research offered a new perspective to explore all types of biochar in wood-plastic composites. However, limited research addressed the difference in the composite mechanical behaviors from PLA and LW after biochar treatment.

As mentioned above, the addition of biochar has a positive effect on the performance enhancement of WPC composites and can improve the strength of the composites, but the influence of biochar content and particle size may have a negative impact on the performance of the composites. At present, the performance optimization of composites is mainly carried out through repeated experiments, which is a time-consuming and laborious process and wastes raw materials, so the researchers established a prediction model through the relationship between some production parameters and properties of composites. Sun et al. used the genetic algorithm and artificial neural network to predict the properties of WPC composites, and the results showed that the optimized model could effectively predict the properties of the composites (Sun et al., 2012). Xu et al. studied the changes of mechanical properties of WPC composites when the different sizes of wood fibers were mixed by combining experiment and numerical modeling. The results show that the Rule of Mixtures (ROM) model has higher prediction accuracy (Xu et al., 2023). Feng et al. studied the influence of molding process parameters on the properties of WPC using finite element method, and found that wood powder content had the greatest influence on its properties, followed by temperature, coupling agent content and screw speed (Feng et al., 2023). Ozturk et al. used artificial neural network (ANN) to optimize the molding process and properties of wood veneer/polystyrene composite (WPCP), and analyzed the influence of hot pressing process parameters on the mechanical properties of the composite (Ozturk et al., 2022). Khamtree et al. used the response surface method to optimize the molding process parameters of WPC composites, and used multivariate nonlinear regression to predict the influence of different raw material ratios on the strength of the composites. The results found that the difference between the experimental results and the predicted values was less than 5 %, which proved the accuracy of the model (Khamtree et al., 2023). However, there is no literature report on the prediction model between the reinforcement phase parameters (content and particle size) and the properties of prepared composites.

Hence, it is crucial to investigate the different biochar contents and particle sizes on the mechanical properties of new types of LW/PLA composites, as well as possible mechanisms. First, LW and PLA were manufactured as a composite matrix. Biochar content and particle size were used as variables. Then, changes in mechanical properties, dynamic thermo mechanical analysis and morphological properties were explored. A prediction model for mechanical properties was established, which can better guide the selection of biochar content and particle size. Moreover, the effects of three different temperatures (20°C, 35°C and 50°C) on the water absorption behaviour were investigated. Finally, the microstructure and interface behaviour of composites were analyzed. This study will further our understanding of biochar applications in LW/PLA composites, and provide basic data for their use in sustainable development practice.

## 2. Materials and methods

### 2.1. Materials

The LW were collected from a campus program (Shanxi Agriculture University, China). It is mainly poplar branch. Polylactic acid PLA, 4032D was purchased from Huachuang Plastic Products Company (Guangzhou, China). The biochar was purchased through Fujian Xinsen Charcoal (Fujian, China). Four different particle size were labeled as BC-100 (particle size 100 mesh), BC-300 (300 mesh), BC-800 (800 mesh), and BC-1200 (1200 mesh).

### 2.2. Composites preparation

First, LW was prepared by crushing, sieving 100 mesh and drying. PLA, BC and pretreated LW were thoroughly mixed at high speed for 60 s (The ratio of LW to PLA is 4:6, and the ratio of biochar is the percentage of the sum of the two). Then, the homogeneous mixture was passed through a SJ35 single-screw extruder (Jiangyin Lianli Plastic Machinery Company, China), at a speed of 30 r/min. The extruder had three temperature control zones set at 50 ℃/145 ℃/155 ℃. The extruded material was sheared into pellet size, molded on a flatbed vulcanizing machine,and then cut into samples using a miniature table saw.

In this study, The LW/PLA composites without biochar was mixed using the same process, and served as a control. The composites preparation process is illustrated in Fig. 1. The formulation of LW/PLA composites is shown in Table 1.

### 2.3. Mechanical properties testing

Flexural properties were measured at a speed of 5 mm/min on an STD-500 electronic universal testing machine (XiaMen YiShiTe Instruments Co., Ltd. China) according to the ASTM D790–10. Rectangular specimens with 80 mm × 12.7 mm × 2.2 mm were tested. Impact strength were performed on an XJJ5 beam impact testing matchine (Chengde Kecheng Testing Machine,China) according to the ASTM D6110–10. The test samples were 125 mm × 12.7 mm × 2 mm. All tests were measured at an room temperature of 20℃. Tests were measured five times, and mean values were obtained.

### 2.4. Water absorption test

Water absorption test of the composites was conducted (ASTM D 570–98), and the sample size was 76 mm×25 mm×2 mm. Firstly, the specimen was dried in a blast oven at 110°C for 8 hours, and the initial mass ($m_0$) was weighed. Then the composites were immersed into the water bath at 20°C. The specimens were taken out after every certain time, and wiped off with filter paper and weighted. Test were repeated, until the composite material is saturated with water absorption. The water absorption percentage ($M_t$) was calculated using Eq. (1):

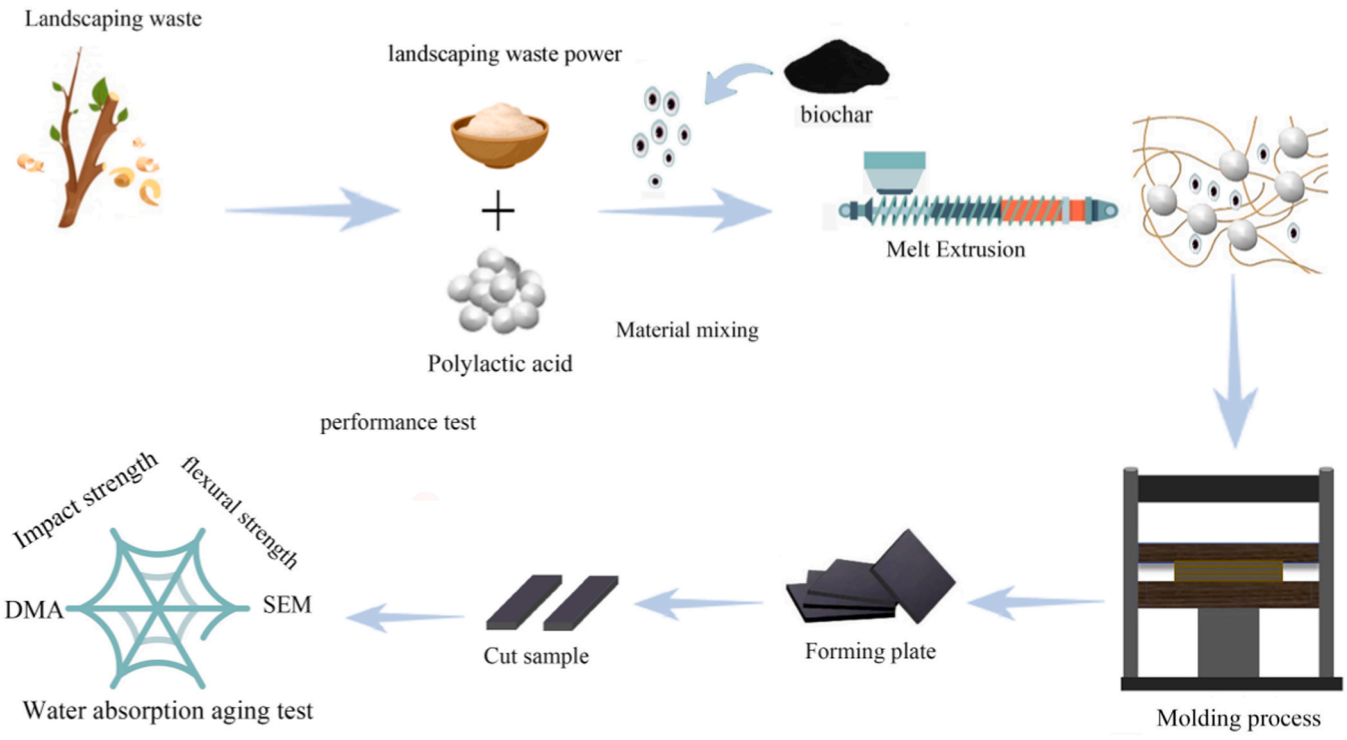


**Fig. 1.** Preparation process of biochar reinforced LW/PLA composites.

**Table 1**
Formulation of LW/PLA composites.

| Number | PLA (%) | LW (%) | Biochar (%) | Biochar particle size (mesh) |
|---|---|---|---|---|
| 1 | 60 | 40 | 0 | – |
| 2 | 59.5 | 40 | 0.5 | 100 |
| 3 | 59 | 40 | 1 | 100 |
| 4 | 58 | 40 | 2 | 100 |
| 5 | 57 | 40 | 3 | 100 |
| 6 | 56 | 40 | 4 | 100 |
| 7 | 59 | 40 | 1 | 300 |
| 8 | 59 | 40 | 1 | 800 |
| 9 | 59 | 40 | 1 | 1200 |

$$M_t = \frac{m_t - m_0}{m_0} \times 100\% \quad (1)$$

Where $m_0$ is the weight of the specimen before water absorption at $t = 0$; $m_t$ is the weight of the specimen for $t$ time after immersion.

The water absorption thickness swelling (TS) was calculated using Eq. (2):

$$TS = (H_t - H_0) \times 100\%/H_0(\%) \quad (2)$$

Where: $TS$ is the expansion rate of water-absorbing thickness at time $t$; $H_0$ is the thickness of the specimen before water absorption (mm); $H_t$ is the thickness of the specimen at time $t$ after immersion (mm).

The water absorption behaviour of wood composite is closely related to the environment temperature. Therefore, the diffusion law of LW/PLA composites with 1 % BC was investigated at different temperatures (20°C, 35°C and 50°C). Briefly, all these specimens were also immersed in three different water baths, respectively. Five specimens from every group were measured, and the mean values were retained.

### 2.5. Dynamic thermomechanical analysis (DMA)

Dynamic thermal mechanical behaviour of samples were conducted by DMA TAQ800 (TA, USA). The energy storage modulus (E′), loss modulus (E″) and loss angle tangent (tanδ) of the composites were measured. Tests were carried out using the temperature sweep mode with a constant frequency of 1 Hz. The temperature range was from 25 °C to 150 °C.

### 2.6. SEM analysis

The morphology and fracture surfaces of composites were characterized using scanning electron microscopy (Zeiss, Sigma-300, Germany), at an operating voltage of 3.0 kV. For SEM observation, all specimen were gold sputtered on the surface before examination. The micro structure of composite samples were observed before and after water absorption.

## 3. Results and analysis

### 3.1. Effect of biochar content and particle size on mechanical properties of LW/PLA composites

The composites without BC were used as the control, and different BC contents on the mechanical properties of LW/PLA composites is shown in Fig. 2.

The incorporation of biochar enhanced the flexural properties of the composites compared to control group without BC addition (Fig. 2a). With 1 % BC addition, the flexural strength reached 25.16 MPa, an increased of 19.20 % and an increase in the elastic modulus by 10.52 %, compared to the control composites without BC addition. Biochar had a certain degree of stiffness and rigidity, composites with a higher BC proportion exhibited greater stiffness and incresed flexural strength. From the Fig. 3, It has been demonstrated that biochar can fill PLA materials after high temperature melt blending, and then form mechanical interlock, that effectively transfers stresses. This was consistent with the results of previous studies (Arrigo et al., 2020; Shah et al., 2023; Sheng et al., 2022; Wei et al., 2022). As biochar contents increased, both flexural strength and modulus decreased. The excess BC particles led to an uneven dispersion, caused by agglomeration, and impacted the

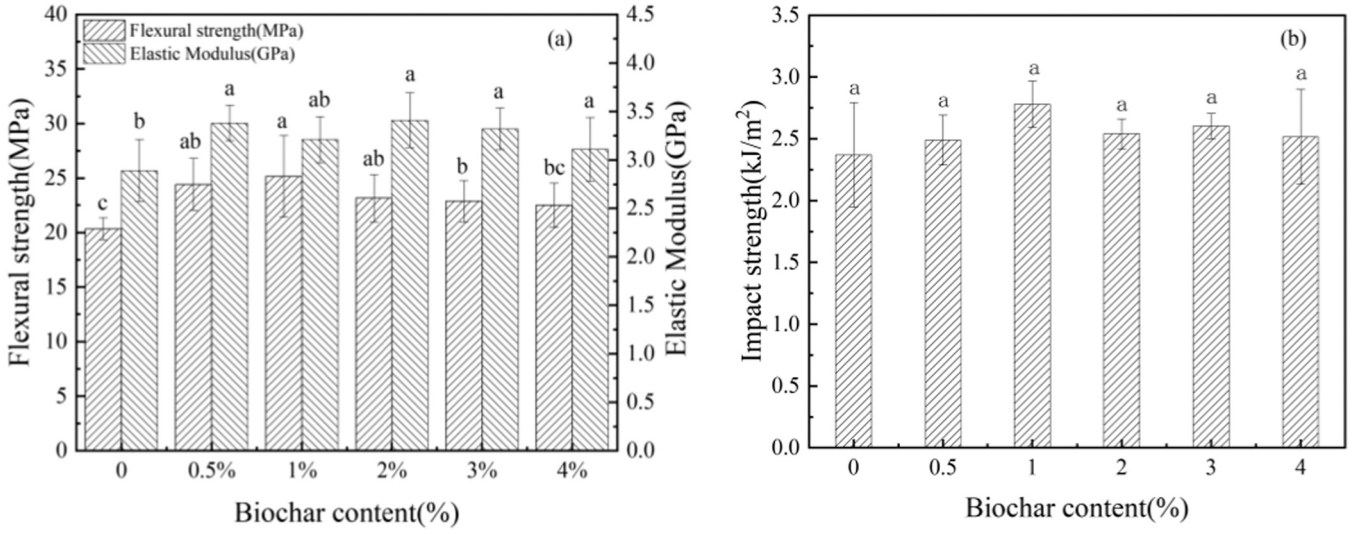


**Fig. 2.** Influence of biochar content on the mechanical properties of composites: (a) Flexural Properties (b) Impact Strength.

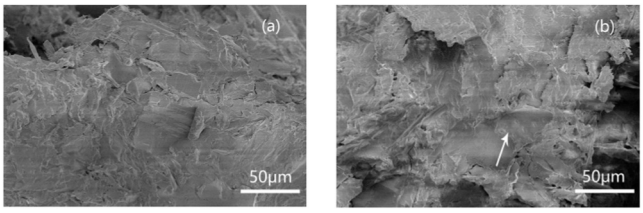


**Fig. 3.** SEM of LW/PLA composites with different biochar contents (a) 0 %, (b) 1 %.

flexural properties. Das et al. also concluded that biochar-reinforced polymer composites have excellent mechanical properties (Das et al., 2021). From Fig. 2b, There was no significantly difference in impact strength for sample.The sample treated with 1 % biochar achieved an impact strength of 2.63 kJ/m$^2$, 3.06 % higher than the control. Overall, the addition of small amounts of biochar (0.5 %BC, 1 %BC) beneficially increased the material stiffness and reduced the toughness, while too much biochar (2 %BC, 3 %BC, 4 % BC) was unfavorable for the impact strength.

The mechanical properties of the composites for different biochar particle size (BC-100, BC-300, BC-800 and BC-1200) are shown in Fig. 4. From Fig. 4a, the flexural strength and modulus of the LW/PLA samples were lower with increasing particle size. The flexural strength and modulus of samples with BC-1200 were reduced by 9.38 % and 12.14 %, compared with the composites made with BC-100. The number of smaller BC particles is greater for the same mass, which may form agglomerates leading to non-uniform dispersion and formation of new stress defects, resulting in reduced composite strength and stiffness. From Fig. 4b, the impact strength of composites decreased with smaller biochar particle size. For BC-1200 composite impact strength was reduced by 26.12 % over BC-100.This was mainly due to the fact that larger biochar particles tend to have a more microporous structure (He et al., 2018). As with the flexural properties, although smaller biochar can fill the pores between LW and PLA better, it was also more susceptible to agglomeration and inhomogeneous dispersion. It is noteworthy that the BC-100 composite had the best mechanical properties. This suggests that 100 mesh biochar could be added into the molten LW/PLA to form a better interfacial connection.

The current study examined how different biochar contents and particle size affect mechanical properties using a single variable experimental approach. In the first experiment, the effect of biochar content

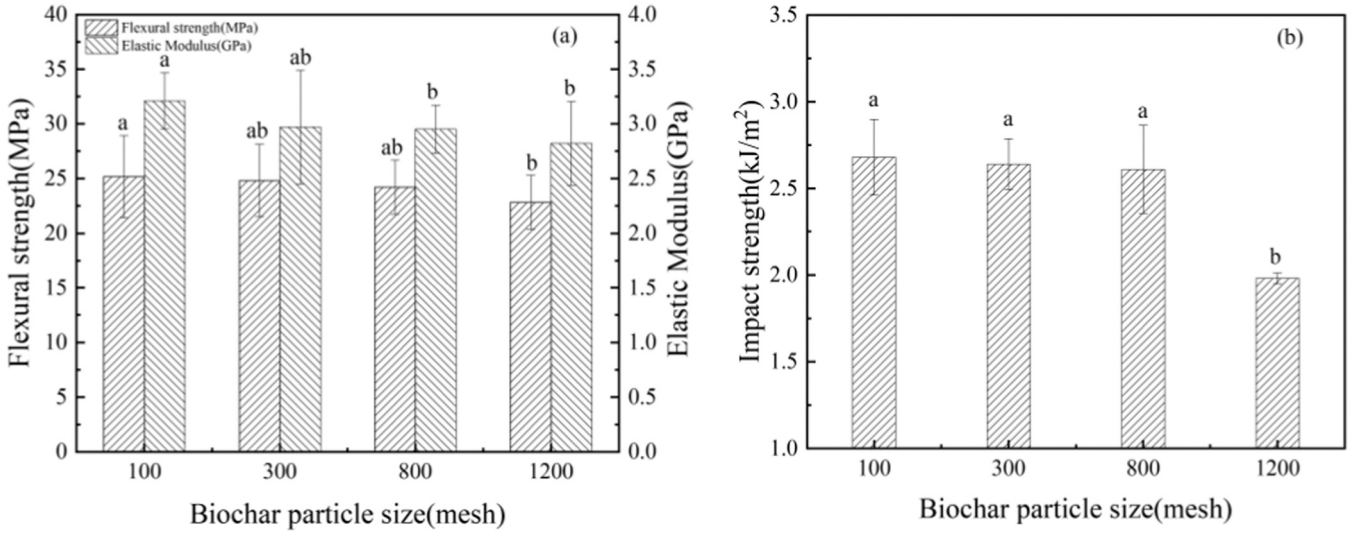


**Fig. 4.** Effect of biochar particle size on the mechanical properties of composites: (a) Flexural Properties (b) Impact strength.

with a constant mesh size (BC100) was investigated. The results showed there was a nonlinear relationship between BC content and flexural strength of the LW/PLA composites. In the second experiment, LW/PLA was combined with 1 % biochar of varying particle sizes. The results showed that BC particle size had a linear relationship with flexural strength. In practical application, there was an interaction between content and particle size. Therefore, a regression model based on these two variable results was investigated to predict the mechanical behaviour of LW/PLA/BC composites. First, a linear regression of flexural strength (Y) versus BC particle size levels (X) was established. Then, the binary nonlinear model was transformed into a linear Eq. (5b) by using Eq. (5a) on the basis of the mechanical property results.

$$Y=\alpha_0+\alpha_{11}X_1+\alpha_{21}X_2+\alpha_{12}X_1^2+\alpha_{22}X_2^2+\alpha_{11\times22}X_1X_2+\omega \quad (5a)$$

Let $\alpha_1=\alpha_{11}$, $\alpha_2=\alpha_{21}$, $\alpha_3=\alpha_{12}$, $\alpha4=\alpha_{22}$, $\alpha_5=\alpha_{11\times22}$, $X_3=X_1^2$, $X4=X_2^2$, and $X_5=X_1X_2$, which translated into a five-element linear regression equation as follows:

$$Y=\alpha_0+\alpha_1X_1+\alpha_2X_2+\alpha_3X_3+_{\alpha4\times4}+\alpha_5X_5+\omega \quad (5b)$$

Where Y is the regression value, i.e., flexural strength, $X_1$ and $X_2$ are the two independent variables, i.e., content of BC and particle size, respectively. $\alpha_0$, $\alpha_1$, $\alpha_2$, $\alpha_3$, $\alpha_4$, and $\alpha_5$ are the biased regression coefficients, and $\omega$ is the random error, with a mean value of zero.

Table 2 shows the raw and linearly transformed data for biochar content and particle size versus flexural strength of composites. The middle data group (group 5) was randomly taken as the validation group, and the other 7 groups of data were brought to build the model. The SPSS results indicated the regression model between composite flexural strength (Y), biochar content ($X_1$) and particle size ($X_2$) as shown below.

$$Y=27.491-2.846X_1+0.406X_1^2-1.528E\text{-}6X_2^2 \quad (6)$$

The fit of the above regression equation was tested. The $R^2$ value of 0.971 indicated that the regression equation fits the data well. From Table 3, P value was less than 0.05, which means that the regression equation was significant, i.e., the establishment of the regression equation was meaningful. Additionally, Table 4 shows significance level of the coefficients $\alpha_1$, $\alpha_3$, and $\alpha_4$ were all below 0.05, indicating that the variables BC content($X_1$) and particle size ($X_2$) had a significant effect on the composite flexural strength (Y).

The predicted and experimental values of flexural strength calculated based on the above regression model are shown in Table 5. The relative errors between predicted and actual values were all controlled within 2 %. The smallest deviation was only 0.22 %, indicating that the prediction model had good credibility. The data from the validation group (0.5 % BC content, 100 mesh particle size) were brought into the regression equation, and the predicted flexural strength was 26.15 MPa. Notably, the actual flexural strength value was 24.42 MPa, with a relative error of 7.1 %, indicating a good prediction.

**Table 2**
Original data and linear transformation data of biochar content and particle size and flexural strength of composites.

| Number | BC content $X_1$ ( % ) | Particle sizes $X_2$ (mesh) | $X_3$ | $X_4$ | $X_5$ | Flexural strengthY ( MPa ) |
|---|---|---|---|---|---|---|
| 1 | 1 | 100 | 1 | 10000 | 100 | 25.16 |
| 2 | 1 | 300 | 1 | 90000 | 300 | 24.8 |
| 3 | 1 | 800 | 1 | 640000 | 800 | 24.2 |
| 4 | 1 | 1200 | 1 | 1440000 | 1200 | 22.8 |
| 5 | 0.5 | 100 | 0.25 | 10000 | 50 | 24.42 |
| 6 | 2 | 100 | 4 | 10000 | 200 | 23.14 |
| 7 | 3 | 100 | 9 | 10000 | 300 | 22.86 |
| 8 | 4 | 100 | 16 | 10000 | 400 | 22.5 |

**Table 3**
Analysis of variance of multivariate linear regression equation.

| model | Sum of Squares | degree of freedom | Mean Square | F | Significance (P) |
|---|---|---|---|---|---|
| Regression | 6.635 | 3 | 2.212 | 33.452 | 0.008 |
| Residual | 0.198 | 3 | 0.066 | | |
| Total | 6.833 | 6 | | | |

**Table 4**
Regression coefficient test of multivariate linear regression equation.

| coefficient | t | Significance (P) |
|---|---|---|
| $\alpha_0$ | 79.762 | < 0.001 |
| $\alpha_2$ ($X_1$) | −4.882 | 0.016 |
| $\alpha_3$ ($X_3$) | 3.399 | 0.042 |
| $\alpha_4$ ($X_4$) | −6.824 | 0.006 |

**Table 5**
Actual and predicted values of composites with different particle sizes and contents.

| Biochar | | Flexural strengthY (MPa) | | Relative error (%) |
|---|---|---|---|---|
| BC content $X_1$ (%) | Particle sizes $X_2$ (mesh) | Actual value | Predicted value | |
| 1 | 100 | 25.16 | 25.04 | 0.47 |
| 1 | 300 | 24.80 | 24.91 | 0.44 |
| 1 | 800 | 24.20 | 24.07 | 0.54 |
| 1 | 1200 | 22.80 | 22.85 | 0.22 |
| 2 | 100 | 23.14 | 23.41 | 1.17 |
| 3 | 100 | 22.86 | 22.59 | 1.18 |
| 4 | 100 | 22.50 | 22.59 | 0.40 |

### 3.2. *Effect of biochar content on water absorption properties of LW/PLA composites*

To gain a deeper understanding of the long-term dimensional stability of LW/PLA composites in aqueous environments, the water-absorption rate and water-absorption expansion rate in the thickness directions were investigated. From Fig. 5, the water absorption of LW/PLA composites increased progressively with increasing immersion time in water. However, the slope gradually decreased, indicating that the growth rate tended to flatten out. From Fig. 5a, all BC addition reduced water absorption, compared to the control sample without biochar. In the 1 % BC composite sample,water absorption was reduced by 6.14 % compared to the control composites. This reduction was mainly because BC particles filled the tiny pores in the interfacial bond between LW/PLA, with the BC addition. From Fig. 5b, the thickness expansion of water absorption gradually decreased with increasing BC content and was lowest at 4 %. This indicated that biochar positively affected the dimensional stability of LW/PLA composites. On the one hand, the BC strengthened the matrix interfacial bonding, and allowed fewer water molecules to penetrate into their interior. On the other hand, the water absorption deformation of wood fiber was inhibited by PLA and BC, these enabled the composite to resist swelling better in the thickness direction after water absorption (Hoang et al., 2024). However, the water absorption rate of LW/PLA composites were not increase as significantly with the addition of biochar as the thickness expansion rate. This could be due to that excessive amount of BC cannot be uniformly distributed within the LW/PLA composites, resulting in agglomeration of BC particles. The internal porosity of the composites increased, allowing water molecules to penetrate more easily. In terms of cell structure, this was due to that poplar fibers have more vessel, larger cell cavities and thinner cell walls, which allows free water to easily enter the cell cavity for storage and to bind to hydroxyl groups on the cell wall (Pan et al. 2024).

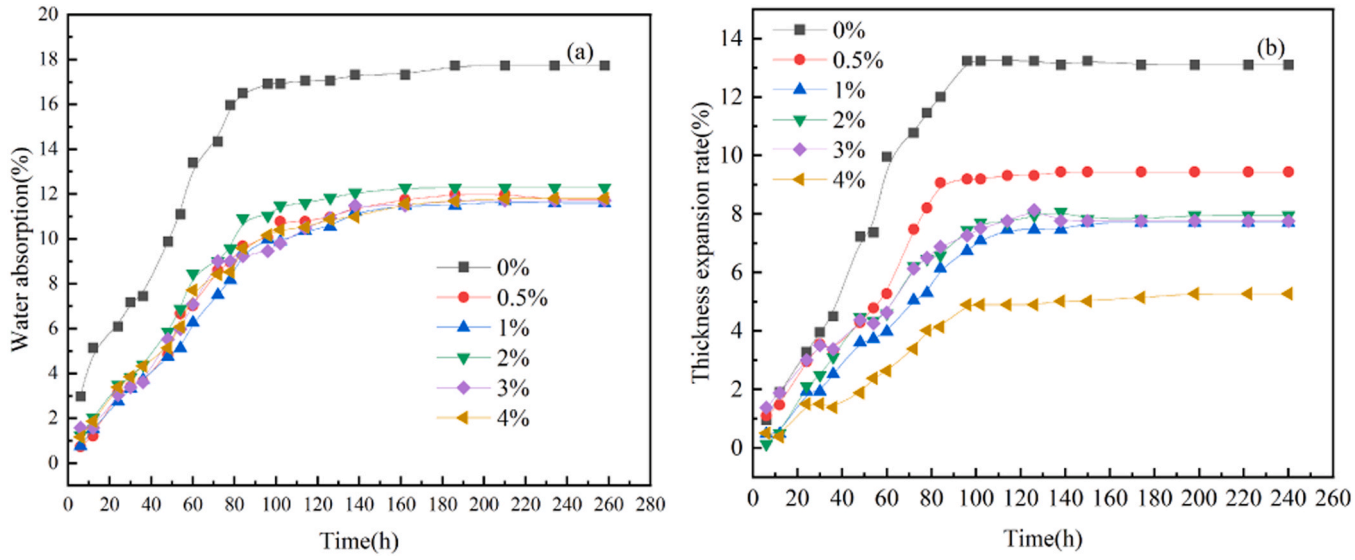


**Fig. 5.** Water absorption properties of LW/PLA composites with different BC contents: (a) Water absorption(b) Thickness expansion rate.

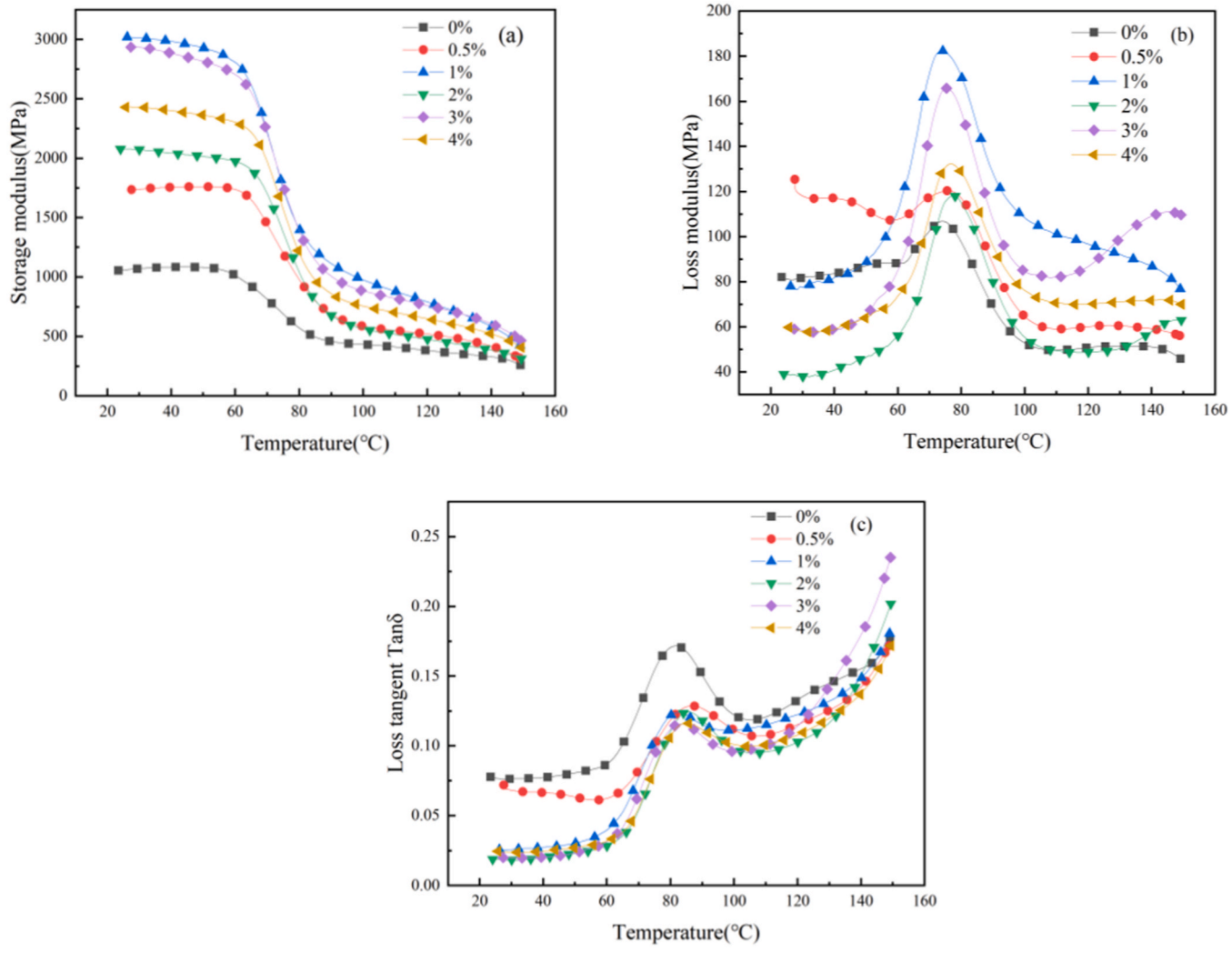


**Fig. 6.** Dynamic thermo-mechanical analysis curves of LW/PLA composites with different biochar contents: (a) storage modulus E′(b) loss modulus E"(c) loss factor tanδ.

### 3.3. Effect of biochar content on dynamic thermo-mechanical properties of composites

DMA was utilized to characterize the dynamic thermo-mechanical properties of the materials. From Fig. 6a, the storage modulus of all LW/PLA composites increased after adding the biochar. This indicated that the addition of biochar in the composite material increased the material's load-bearing capacity. Also, increasing the temperature led to an increase in the storage modules. Earlier studies showed that the molecular activity of the PLA chain increased at higher temperatures (Esmizadeh et al., 2019; Hassan et al., 2019). After 1 %BC addition, the E′(max) reached 3018 MPa, 65 % higher than the pure LW/PLA composite. From Fig. 6b, the results exhibited a similar trend to the storage modulus results. Samples with 1 %BC had the highest loss modulus value. As mentioned above, a strong interfacial bonding was formed after 1 %BC addition, which could effectively transfer stress and improve toughness (Essabir et al., 2018). The changes in loss factor tanδ of all the composites are shown in Fig. 6c. The loss coefficient reflects the viscosity characteristics of materials and the mobility of polymer segments. Among them, the larger the peak value of tanδ, the greater the internal friction of the material, and the poorer the internal bonding strength of the corresponding material, and vice versa(Ornaghi et al., 2010). More biochar addition led to a restriction or narrowing of the polymer segments, which affected the mobility and $T_g$ value of polymer segments. After adding BC, the peak values of BC composites decreased, the glass transition temperature shifted to the right. The $T_g$ value increased compared to the composites without BC, which indicated that the internal friction of the composites with BC was low, and the internal bonding strength was higher than that of the samples without BC.

### 3.4. Study of water absorption behavior of LW/PLA composites

The mechanical properties of composites during water absorption are influenced by the environmental temperature and immersion time. The water absorption behavior of LW/PLA samples with 1 % BC was analyzed at 20℃, 35℃ and 50℃, respectively. From Fig. 7, the saturated water absorption ($M_m$) of the composites in 50℃ water was significantly higher than in 20℃ and 35℃ water, indicating higher temperature led to increased $M_m$ value. At temperatures of 20℃ and 35℃, the water absorption rate of LW/PLA samples initially increased. In the second phase, it then decreased significantly, with the weight increasing slightly, until equilibrium was reached. Conversely, at 50°C, the composites exhibited faster water absorption.

Moisture diffusion primarily follows Fickian diffusion, non-Fickian diffusion (irregular diffusion) or a combination of both (Scida et al., 2013). The moisture diffusion law of a material can be described by the kinetic equation (Assarar et al., 2011):

$$\frac{M_t}{M_m} = kt^n \tag{7}$$

Where: $M_t$ is the weight gain of the material at moment t, $M_m$ is saturated water absorption, $k$ and n are diffusion kinetic parameters.

When the value of n is about 0.5, it is found that the diffusion behavior of water molecules within the material follows Fickian's diffusion law (Espert et al., 2004; Petchwattana et al., 2013). Then, taking the logarithms on both sides of equal Eq. (7), it can be described by the following equation:

$$\log\left(\frac{M_t}{M_m}\right) = \log(k) + n\log(t) \tag{8}$$

Figs. 8 and 9 show the fitted water absorption data for LW/PLA samples and their comparison with the Fickian model. It was note that, the n value of the diffusion kinetic parameter for LW/PLA composites were close to 0.5 at all three water temperatures, indicating that the pre-absorption behavior of LW/PLA composites followed Fickian water absorption model (Saikia, 2010). Following that, the diffusion coefficient (D) and $M_m$, can be calculated as Equation (Cheng et al., 2021):

$$D = \frac{\pi}{(4M_m)^2} \times \left(\frac{M_t \times h}{\sqrt{t}}\right)^2 = \frac{\pi k'^2}{(4M_m)^2} \tag{9}$$

Where: h is the thickness of the specimen (mm); the coefficient k ' is the slope of the linear part of the curve $M_t = f(\sqrt{t}/h)$.

The water diffusion coefficients D of LW/PLA composites at 20℃, 35°C and 50°C are shown in Table 6. The diffusion coefficient increased from $3.26\times10^{-6}$ $mm^2/s$ (20°C) to $3.83\times10^{-6}$ $mm^2/s$ (50°C). In general, the higher the diffusion coefficient, the weaker the adhesion interface between resin and fiber, and the more difficult it was for water to diffuse in the composite. Higher temperatures reduced the adhesion between LW/PLA and biochar, and the equilibrium time of water uptake decreased accordingly.

As mentioned above, heating can accelerate the diffusion process, and the water molecules in LW/PLA/BC composites were the thermally activated factor. For Fick diffusion, the diffusion coefficient versus temperature can be expressed by the Arrhenius equation (Liu et al., 2022), which is shown in (10):

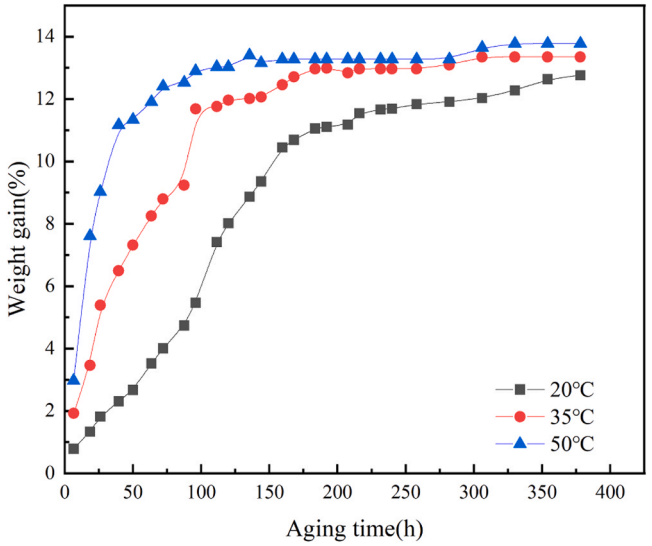


**Fig. 7.** Weight gain curves of LW/ PLA composites at 20℃, 35℃and 50℃.

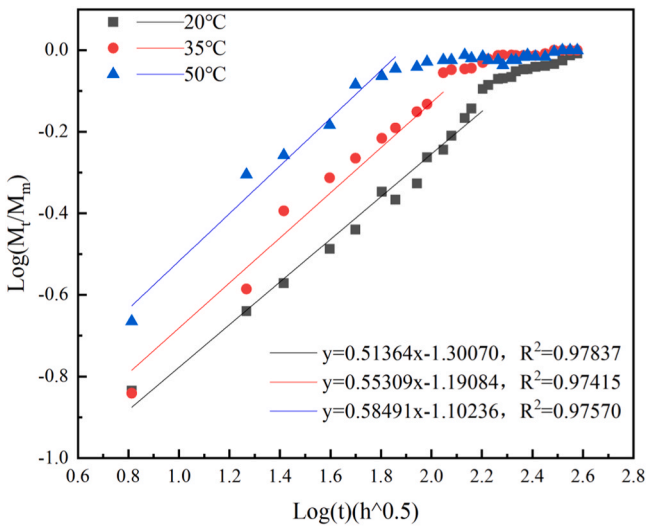


**Fig. 8.** Diffusion curve fitting of LW/PLA composites at 20℃, 35℃ and 50℃.

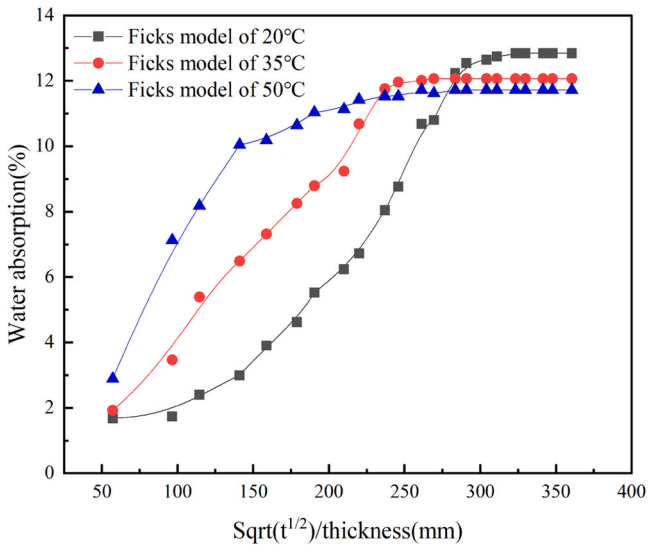


**Fig. 9.** Fitting of LW/PLA composite Fickian model at 20℃, 35℃ and 50℃.

**Table 6**
Dynamic parameters and diffusion coefficients of WF/PLA composites at different temperatures.

| Type | n | k | $R^2$ | $D\times10^{-6}$ ($mm^2/s$) |
|---|---|---|---|---|
| 20℃ | 0.51364 | 0.05201 | 0.95656 | 3.26 |
| 35℃ | 0.55309 | 0.05681 | 0.98572 | 3.55 |
| 50℃ | 0.58491 | 0.05345 | 0.91486 | 3.83 |

$$D = Ae^{-\frac{E}{RT}} \tag{10}$$

where D is the permeability index ($mm^2/s$), E is the activation energy of the diffusion process (kJ/mol), and R is the ideal gas constant (8.314 J/mol·K).

Taking logarithms on both sides of Eq. (10) yields:

$$\ln D = \ln A - \frac{E}{RT} \tag{11}$$

LnD and (1/T) are linearly related, and the values of diffusion coefficients at different environmental temperatures are substituted into Eq. (11). Next, a one-way linear regression can be performed. The fitting results are shown in Fig. 10, yielding the predictive model function $D=2.44\times10^{-5}$ exp (-435.31/T) for the water molecule diffusion coefficient of LW/PLA composites, which predicts the water diffusion coefficient D at any water immersion temperature.

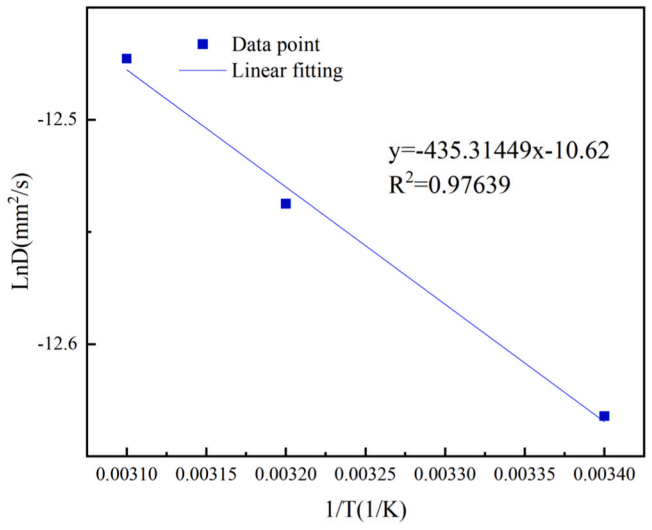


**Fig. 10.** Arrhenius logarithmic fitting curve of diffusion coefficient of LW/PLA composites at 20℃, 35℃ and 50℃.

Finally, the predicted value and experimental data for LW/PLA composites at temperature 60 ℃ were tested. According to Fick's law, the diffusion coefficient D is $6.90\times10^{-6}$ $mm^2/s$, and the prediction model estimates D at $6.61\times10^{-6}$ $mm^2/s$, with an error of 4.45 %.

### 3.5. Scanning electron microscopy (SEM)

The microstructures of all LW/PLA samples under three different temperature conditions are shown in Fig. 11. For the micro structure of LW/PLA composites before water absorption (Fig. 11a), the cross-section morphology was concave-convex and rough, and no cracks were clearly visible. There was good interfacial compatibility between the composite and BC, which effectively enabled stress transfer and reinforcement by the BC particle. As shown in Fig. 11 b-d, water absorption caused local debonding within the particle matrix with small fissures indicating weaken inter facial bonding. At 35°C, water absorption led to crack formation on the fracture surfaces, and as the fissures expanded, more significant damage occurred at the interface within LW/PLA composites. At temperature of 50°C, increased crack porosity and deepened fractures were observed. The penetration of additional water molecules led to molecular chain hydrolysis. With the combined effects of oxygen and heat, higher water temperatures and longer durations resulted in greater water absorption and an increased water diffusion rate. In addition, the difference in expansion rates between the LW fibers and PLA generated inconsistent forces at the interface. Consequently, a weakened interfacial zone formed, which led to increased cracking and degradation between the LW and the PLA matrix.

## 4. Conclusions

With varying biochar content and particle size, LW/PLA/BC were manufactured using extrusion and molding process. The incorporation of biochar enhanced the mechanical properties and reduced the water absorption of the composites. A 1 % addition of biochar led to a 19.20 % increase in flexural strength and a 3.06 % rise in impact strength. However, excessive biochar content (2 %, 3 %,4 %) led to a decline in mechanical properties. Then, a regression model was able to predict the flexural strength based on biochar particle size and content, achieving an accuracy of 99.37 %. Dynamic thermo-mechanical analysis revealed that BC improved the storage modulus of LW/PLA samples, indicating enhanced interfacial interaction between LW and PLA.

Water-absorption aging test was carried out on composites with different biochar contents. Adding 1 % biochar significantly reduced water absorption and effectively strengthened the bonding between LW fibers and PLA matrix. Additionally, the initial water diffusion behaviour of the composites followed the Fickian diffusion mode, where higher temperature accelerated water diffusion and increased the equilibrium water absorption. SEM showed that higher temperature resulted in more severe the damage at the interface of the composites, indicating accelerated degradation of the composites. In combination with the Arrhenius equation, a predictive model function was developed, to estimate the water diffusion coefficient D at various temperature. The proposed model function can better predict the water absorption diffusion coefficient of this composite at 60°C water immersion temperature.

## CRediT authorship contribution statement

**Ruyan Zhang**: Writing – original draft, Methodology, Investigation, Formal analysis. **Haixin Peng**: Writing – review & editing, Conceptualization. **Shenhao Li** & **Xia Yang**: Data curation, Conceptualization.

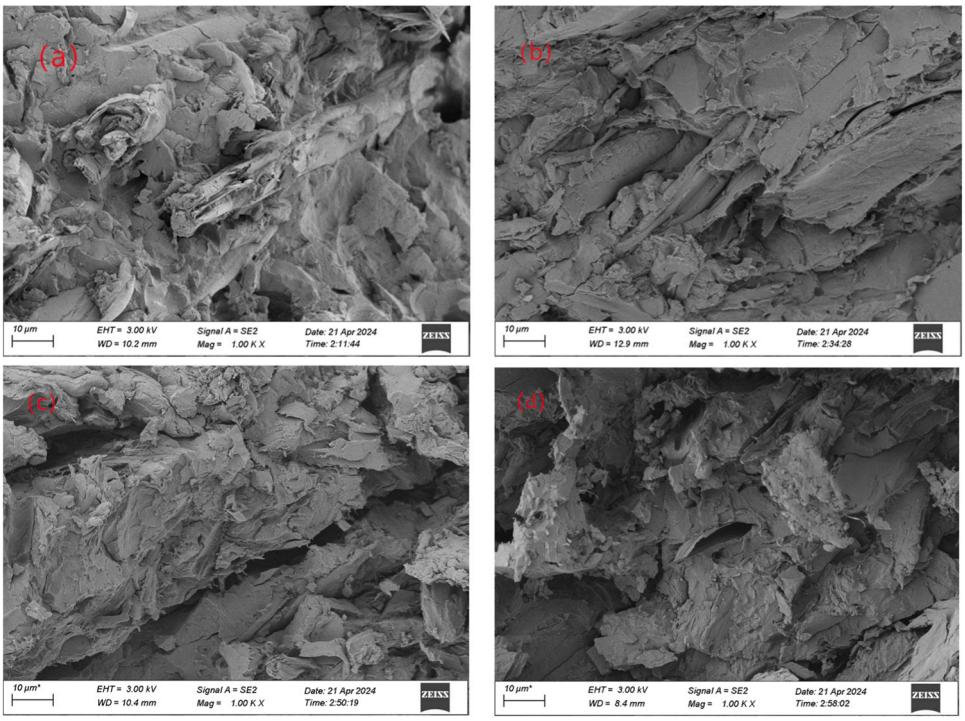


**Fig. 11.** SEM images of LW/PLA composites at different temperatures: (a) before water absorption (b) 20℃ water environment (c)35℃ water environment (d)50℃ water environment.

**Hongbo Li**: Validation, Methodology. **Zebing Xing**: Validation, Methodology. **Yu xian**: Writing – review & editing, Supervision, Conceptualization, Project administration.

## Declaration of Competing Interest

The authors declare that they have no known competing financial interests or personal relationships that could have appeared to influence the work reported in this paper.

## Acknowledgments

The authors gratefully acknowledge to the Fundamental Research Program of Shanxi Province (No. 202303021221090), Research Project of the Shanxi Scholarship Council of China (No. 2021-075). The authors extend their gratitude to Ms. Zhang from Shiyanjia Lab (www.shiyanjia.com) for providing invaluable assistance with the SEM and DMA analysis.

## Data availability

The authors do not have permission to share data.

## References

An, L., 2020. The method for static composting treatment of the landscaping waste. Front. Energy Res. 8. https://doi.org/10.3389/fenrg.2020.00024.

Arrigo, R., Bartoli, M., Malucelli, G., 2020. Poly (lactic acid)–biochar biocomposites: effect of processing and filler content on rheological, thermal, and mechanical properties. Polymers 12 (4), 892. https://doi.org/10.3390/polym12040892.

Assarar, M., Scida, D., Mahi, A.E., Poilane, C., Ayad, R., 2011. Influence of water ageing on mechanical properties and damage events of two reinforced composite materials: flax–fibres and glass–fibres. Mater. Des. 32 (2), 788–795. https://doi.org/10.1016/J.MATDES.2010.07.024.

Bai, J., Shen, H., Dong, S., 2010. Study on eco-utilization and treatments of highway greening waste. Procedia Environ. Sci. 2, 25–31. https://doi.org/10.1016/j.proenv.2010.10.005.

Cheng, Z., Kong, F., Zhang, X., 2021. Application of the Langmuir-type diffusion model to study moisture diffusion into asphalt films. Constr. Build. Mater. 268, 121192. https://doi.org/10.1016/j.conbuildmat.2020.121192.

Chong, W.J., Shen, S., Li, Y., Trinchi, A., Pejak, D., Kyratzis, I.L., Sola, A., Wen, C., 2021. Additive manufacturing of antibacterial PLA-ZnO nanocomposites: benefits, limitations and open challenges. J. Mater. Sci. Technol. (16), 32. https://doi.org/10.1016/j.jmst.2021.09.039.

Das, C., Tamrakar, S., Kiziltas, A., Xie, X., 2021. Incorporation of biochar to improve mechanical, thermal and electrical properties of polymer composites. Polymers 13 (16), 2663. https://doi.org/10.3390/polym13162663.

Esmizadeh, E., Sadeghi, T., Vahidifar, A., Naderi, G., Ghoreishy, M.H.R., Paran, S.M.R., 2019. Nano graphene-reinforced bio-nanocomposites based on NR/PLA: the morphological, thermal and rheological perspective. J. Polym. Environ. 27, 1529–1541. https://doi.org/10.1007/s10924-019-01450-x.

Espert, A., Vilaplana, F., Karlsson, S., 2004. Comparison of water absorption in natural cellulosic fibres from wood and one-year crops in polypropylene composites and its influence on their mechanical properties. Compos. Part A: Appl. Sci. Manuf. 35 (11), 1267–1276. https://doi.org/10.1016/j.compositesa.2004.04.004.

Essabir, H., Raji, M., Laaziz, S.A., Rodrique, D., Bouhfid, R., Qaiss, A. e k, 2018. Thermo-mechanical performances of polypropylene biocomposites based on untreated, treated and compatibilized spent coffee grounds. Compos. Part B: Eng. https://doi.org/10.1016/J.COMPOSITESB.2018.05.020.

Feng, L., Wang, D., Yan, J., 2023. Reliability study of wood–plastic composites based on probabilistic finite elements. Polymers 15, 312. https://doi.org/10.3390/polym15020312.

Fortini, A.M., Valentina, 2018. Combined effect of water uptake and temperature on wood polymer composites. J. Appl. Polym. Sci. 135 (35a36). https://doi.org/10.1002/APP.46674.

Friedrich, D., 2021. Thermoplastic moulding of Wood-Polymer Composites (WPC): a review on physical and mechanical behaviour under hot-pressing technique. Compos. Struct. 262, 113649. https://doi.org/10.1016/j.compstruct.2021.113649.

George, J., Jung, D., Bhattacharyya, D., 2023. Improvement of electrical and mechanical properties of PLA/PBAT composites using coconut shell biochar for antistatic applications. Appl. Sci. 13 (2), 902. https://doi.org/10.3390/app13020902.

Hassan, M.M., Le Guen, M.J., Tucker, N., Parker, K., 2019. Thermo-mechanical, morphological and water absorption properties of thermoplastic starch/cellulose composite foams reinforced with PLA. Cellulose 26 (7), 4463–4478. https://doi.org/10.1007/s10570-019-02393-1.

He, P., Liu, Y., Shao, L., Lü, H., 2018. Particle size dependence of the physicochemical properties of biochar. Chemosphere. https://doi.org/10.1016/j.chemosphere.2018.08.106.

Hoang, P., Zhang, Z., Ren, J., Peng, Y., Cao, J., 2024. Versatile biochar for wood-plastic composites: improving mechanical properties, dimensional and thermal stability (n/a(n/a)). Polym. Compos.. https://doi.org/10.1002/pc.28477.

Jamshidian, M., Tehrany, E.A., Imran, M., Jacquot, M., Desobry, S., 2010. Poly-lactic acid: production, applications, nanocomposites, and release studies. Compr. Rev. Food Sci. Food Saf. 9 (5), 552–571. https://doi.org/10.1111/j.1541-4337.2010.00126.x.

Khamtree, S., Homkhiew, C., Srivabut, C., Ratanawilai, T., Rawangwong, S., Hiziroglu, S., 2023. Evaluation of mechanical properties of composites made from

recycled plastic and waste rubberwood using multiply-response surface optimization as green building materials. Fibers Polym. 24 (8), 2819–2834. https://doi.org/10.1007/s12221-023-00266-w.
Li, X., Lei, B., Lin, Z., Huang, L., Tan, S., Cai, X., 2014. The utilization of bamboo charcoal enhances wood plastic composites with excellent mechanical and thermal properties. Mater. Des. 53, 419–424. https://doi.org/10.1016/j.matdes.2013.07.028.
Liu, Z., Wang, H., Yang, L., Du, J., 2022. Research on mechanical properties and durability of flax/glass fiber bio-hybrid FRP composites laminates. Compos. Struct. 290, 115566. https://doi.org/10.1016/j.compstruct.2022.115566.
Ma, X., Wang, J., Li, L., Wang, X., Gong, J., 2024. Co-pyrolysis model for polylactic acid (PLA)/wood composite and its application in predicting combustion behaviors. Renew. Energy 225, 120267. https://doi.org/10.1016/j.renene.2024.120267.
Martinez Villadiego, K., Arias Tapia, M.J., Useche, J., Escobar Macías, D., 2022. Thermoplastic Starch (TPS)/Polylactic Acid (PLA) blending methodologies: a review. J. Polym. Environ. 30 (1), 75–91. https://doi.org/10.1007/s10924-021-02207-1.
Mokhtar, N., Razali, S.M., Sulaiman, M.S., Edin, T., Wahab, R., 2022. Converting wood-related waste materials into other value-added products: a short review. IOP Conf. Ser.: Earth Environ. Sci. 1053 (1), 012030. https://doi.org/10.1088/1755-1315/1053/1/012030.
Mølgaard, C., 1995. Environmental impacts by disposal of plastic from municipal solid waste. Resour., Conserv. Recycl. 15 (1), 51–63. https://doi.org/10.1016/0921-3449(95)00013-9.
Ornaghi Jr, H.L., Bolner, A.S., Fiorio, R., Zattera, A.J., Amico, S.C., 2010. Mechanical and dynamic mechanical analysis of hybrid composites molded by resin transfer molding. J. Appl. Polym. Sci. 118 (2), 887–896. https://doi.org/10.1002/app.32388.
Ozturk, H., Demir, A., Demirkir, C., 2022. Optimization of pressing parameters for the best mechanical properties of wood veneer/polystyrene composite plywood using artificial neural network, 2022 Eur. J. Wood Wood Prod. 80 (4), 907–922. https://doi.org/10.1007/s00107-022-01818-2.
Pan, F., Chen, Z., Huang, Y., Xie, J., Jia, H., Jiang, P., 2024. Experimental evaluation of combustion performance in the three main anatomical sections of poplar wood. Wood Mater. Sci. Eng. 1–9. https://doi.org/10.1080/17480272.2024.2320739.
Petchwattana, N., Covavisaruch, S., Pitidhammabhorn, D., 2013. Influences of water absorption on the properties of foamed poly(vinyl chloride)/rice hull composites. J. Polym. Res. 20. https://doi.org/10.1007/s10965-013-0172-y.
Rajeshkumar, G., Seshadri, S.A., Devnani, G.L., Sanjay, M.R., Anuf, A.R., 2021. Environment friendly, renewable and sustainable poly lactic acid (PLA) based natural fiber reinforced composites – A comprehensive review. J. Clean. Prod. 310 (1)), 127483. https://doi.org/10.1016/J.JCLEPRO.2021.127483.
Ramesh, P., Prasad, B.D., Narayana, K.L., 2020. Effect of MMT clay on mechanical, thermal and barrier properties of treated aloevera fiber/ PLA-hybrid biocomposites. Silicon 12 (7), 1751–1760. https://doi.org/10.1007/s12633-019-00275-6.
Ratanawilai, T., Srivabut, C., 2021. Physico-mechanical properties and long-term creep behavior of wood-plastic composites for construction materials: effect of water immersion times. Case Stud. Constr. Mater. https://doi.org/10.1016/j.cscm.2021.e00791.
Saeed, U., Taimoor, A.A., Rathur, S.U., Alhumade, H., AlTuraif, H., Bamufleh, H.S., Al-Zaitone, B., 2023. Sustainable jute fiber reinforced polylactic acid composite: thermochemical and thermomechanical characteristics. J. Compos. Mater. 57 (7), 1363–1376. https://doi.org/10.1177/00219983231152552.
Saikia, D., 2010. Studies of water absorption behavior of plant fibers at different temperatures. Int. J. Thermophys. 31 (4), 1020–1026. https://doi.org/10.1007/s10765-010-0774-0.
Scida, D., Assarar, M., Poilane, C., Ayad, R., 2013. Influence of hygrothermal ageing on the damage mechanisms of flax-fibre reinforced epoxy composite. Compos. Part B Eng. 48, 51–58. https://doi.org/10.1016/j.compositesb.2012.12.010.
Shah, A. u R., Imdad, A., Sadiq, A., Malik, R.A., Alrobei, H., Badruddin, I.A., 2023. Mechanical, thermal, and fire retardant properties of rice husk biochar reinforced recycled high-density polyethylene composite material. Polymers 15 (8), 1827. https://doi.org/10.3390/polym15081827.
Sheng, K., Zhang, Q., Wei, Y., 2022. Effect of biochar on mechanical properties of zein/polypropylene composites. J. Agric. Sci. Technol. 24 (10), 161–168. https://doi.org/10.13304/j.nykjdb.2022.0572.
Song, M.H., 2020. A study on IoT based real-time plants growth monitoring for smart garden. Inst. Internet, Broadcast. Commun. (1). https://doi.org/10.7236/IJIBC.2020.12.1.130.
Sun, J.P., Wang, F.H., Li, P., Cai, Z., 2012. Application of Genetic Algorithm and Artificial Neural Network on Performance Prediction of Wood-Plastics Composite Material. Polym. Mater. Sci. Eng. 28 (1), 117–120. DOI：CNKI:SUN:GFZC.0.2012-01-034.
Wang, L., Wang, T., Hao, R., Wang, Y., 2023. Synthesis and applications of biomass-derived porous carbon materials in energy utilization and environmental remediation. Chemosphere 339, 139635. https://doi.org/10.1016/j.chemosphere.2023.139635.
Wei, Y.-y, Zhang, Q.-f, Sheng, K.-c (2022). Effect of biochar on mechanical properties of zein/polypropylene composites.doi: 10.13304/j.nykjdb.2022.0572.
Xian, Y., Wang, C., Wang, G., Leemiller, S., Cheng, H., 2022. The influence of white mud on the water absorption, surface wettability, mechanical, and dynamic thermomechanical properties of core-shell structured wood-plastic composites. Eur. J. wood wood Prod. 80 (2), 355–365. https://doi.org/10.1007/s00107-021-01772-5.
Xu, H., Yang, Y., Li, L., Liu, B., Fu, X., Yang, X., Cao, Y., 2023. Mechanical properties variation in wood-plastic composites with a mixed wood fiber size. Materials 16, 5801. https://doi.org/10.3390/ma16175801.
Yi, Y., Huang, Z., Lu, B., Xian, J., Tsang, E.P., Cheng, W., Fang, Z., 2020. Magnetic biochar for environmental remediation: a review. Bioresour. Technol. 298, 122468. https://doi.org/10.1016/j.biortech.2019.122468.
Zhang, L., Chen, Z., Dong, H., Fu, S., Ma, L., Yang, X., 2021. Wood plastic composites based wood wall's structure and thermal insulation performance. J. Bioresour. Bioprod. 6 (1), 65–74. https://doi.org/10.1016/j.jobab.2021.01.005.